FARADAY

Dielectric properties of an NaX zeolite as a function of the hydration state

G. Chabanis,[a] A. Abdoulaye,[a] J. C. Giuntini,[a] J. V. Zanchetta,[a]* F. Di Renzo[b] and J. Vanderschueren[c]†

[a] *Laboratoire de Physicochimie de la Matière Condensée, Equipe de Chimie Physique (UMR 5617 CNRS), Université Montpellier II, Pl. Eugène Bataillon, F34095 Montpellier Cedex 5, France*

[b] *Laboratoire de Matériaux Catalytiques et Catalyse en Chimie Organique (UMR 5618), ENSCM, 8, rue de l'Ecole Normale, 34296 Montpellier Cedex 5, France*

[c] *Chimie Macromoléculaire et Chimie Physique, Université de Liège, Institut de Chimie au Sart-Tilman, B4000 Liège, Belgium*

The dielectric properties of the NaX zeolite (Si/Al = 1.3) have been measured after different thermal treatments in the temperature range 100–400 °C. The frequency domain was varied from 10 to 10^6 Hz, the measuring temperature being in the range 80–150 °C. Independent of the outgassing temperature (*i.e.* the number of water molecules), the ac conductivity is ascribed to migration of the supercage cations. The variation in the migration energy (E_{dc}) as a function of the adsorbed water molecules (0.9–0.58 eV) shows their influence on the conduction process. Two relaxation domains are observed: 'low-frequency' and 'high frequency' relaxations, which are due to local hops of cations located in sites II and III, respectively. These two relaxations are confirmed by thermally stimulated current measurements. The energies associated with these relaxations vary with the outgassing temperature.

Introduction

Zeolites are used in industry as adsorbents, ion exchangers, catalysts, molecular sieves, water purifiers *etc.* Other recent applications include batteries, membranes, zeolite–polymer composites, non-linear optical materials, sensors and solar energy converters.[1,2]

The ionic properties of zeolites are connected with their crystalline microporous structure. Their networks have an anionic character,[3] therefore compensating cations, located in channels and cavities of the zeolites, are necessary to preserve the electrical neutrality of the solid.[4] Zeolites also have large interconnected cages which can adsorb water, without changing the silicate network.[5,6]

The dielectric properties are related to different parameters such as the chemical composition (for example Si/Al ratio), the type of exchangeable cations, the degree of crystallinity of the network, the state of hydration and the temperature.[7,8] Dielectric studies have been performed on hydrated and dehydrated samples, leading to hypotheses on the nature of the charge carriers, and on the conduction mechanism.[9–11]

In the case of dehydrated zeolites, it is generally assumed that the extra-network cations are responsible for the process of dielectric relaxation. However, interpretation of the hopping mechanism is still a subject for debate.[12–14] Some authors state that the cationic polarization can be described as the movement of the extra-network cations between different sites.[13,15] However, no model allows the determination of the sites involved in the conduction process, their positions in the structure, or their number.

Identification of the charge carriers responsible for the conduction in the hydrated zeolites remains difficult. Some authors consider that the conduction is mainly due to protons from the adsorbed water,[16,17] whilst others interpret the influence of water in terms of modification of the mobility of these carriers.[13,18]

† Research Associate of the National Fund for Scientific Research (Belgium).

The present work is a contribution to the understanding of the mechanisms of relaxation in a faujasite zeolite. We have studied the influence of adsorbed water on the conductivity, and the relaxation mechanisms of the exchanged cations by means of two complementary techniques of relaxation: complex impedance spectroscopy and thermally stimulated currents (TSC).

Experimental

Conditioning of samples

The NaX zeolite was of commercial origin (faujasite NaX molecular sieve type 13-X from Aldrich). The chemical composition per unit cell (determined by the CNRS, service central d'analyse, Vernaison, France) is $Na_{84}(AlO_2)_{84}(SiO_2)_{108}$, corresponding to a ratio Si/Al = 1.3.

The crystallinity of the sample was examined by X-ray diffraction. The zeolite, in the form of powder (0.15 g), was compressed under a pressure of 3×10^8 Pa in order to obtain cylindrical samples of 13 mm diameter and 1 mm thickness. Electrical contacts were deposited by sputtering a platinum film on the sample plane surfaces. The compactness of the sample is 0.87.

Dielectric measurements

The study of divided solids is still a problem when conductivity measurements are involved. Grain boundary phenomena can occur, especially when an external gaseous phase is used. In fact, when experiments are performed at variable frequency, the only component which appears is the polarization, that depends only on the bulk properties of the solid. The dc measurements can be affected by grain boundary effects. Nevertheless, Freeman *et al.*[18] have shown that the conductivity values measured on zeolites X and Y represent the bulk conductivity.

Concerning the TSC measurements, the method of thermally stimulated polarization current (TSPC) is the natural complement to the thermally stimulated depolarization current (TSDC) technique. It is based on the opposite process,

i.e. measuring the currents generated by the buildup of a polarized state in a dielectric. It has been used, in the following, to check the intrinsic nature of the relaxations observed.

The studied samples were inserted into a measuring cell, in which the sample was dehydrated at the chosen temperature for 24 h under a pressure of 1 Pa. It was found that the dielectric properties did not change when the outgassing time exceeded 18 h, whatever the outgassing temperature.

Parallel measurements of mass loss by thermogravimetric experiments under the same conditions of temperature and pressure allowed determination of the number of water molecules per unit cell (uc), in the zeolite under study, for every outgassing temperature, T_{og}, hence, each T_{og} characterizes a given water content in the solid.

Conductivity

The conductivity measurements were performed under vacuum, as a function of frequency at different temperatures. This was achieved by using an analyser (HP 4192 A) in the frequency range 10 Hz–10 MHz. The input impedance of the analyser was larger than 10 MΩ and its sensitivity was 1.2 pF, allowing an accuracy of 3.5% to be obtained.[19]

In this work, we have studied the evolution of the imaginary part of the electrical permittivity at different T_{og} as a function of frequency and temperature.

TSC/RMA measurements

TSC experiments were also performed on the same samples. They were carried out under helium with a TSC/relaxation map analysis (RMA) spectrometer (Solomat type 91000$^+$) covering the temperature range −170 to 400 °C. This method is described in detail elsewhere.[20,21] We give here some indications of the principle of the TSDC method.

The TSDC method consists of determining, following a strictly controlled temperature programme, the current created by the return to an equilibrium state of a dielectric which has been previously polarized. The following steps of polarization and depolarization are generally necessary when the relaxation spectrum of a material is required in a temperature range T_p–T_0: (i) heating to the polarization temperature T_p; (ii) application of a dc electric field E_p for a time t_p of sufficient duration to obtain saturation of the various polarization processes involved; (iii) rapid cooling in the field to the temperature T_0; (iv) cutting off the external field and linear heating of the short-circuited sample. The TSDC spectrum (*i.e.* current induced by depolarization of the sample during heating) is observed during this last step.

In practice, unless otherwise specified, we have adopted T_p values much lower than T_{og} so that the water content of the sample is not significantly affected during the TSDC run. Other experimental parameters are: $t_p = 2$ min; $T_0 = -160$ °C; $E_p = 3 \times 10^5$ V m^{-1} and b (heating rate) = 10 °C min^{-1}.

The TSDC and TSPC methods are 'global' techniques allowing a complete picture of the temperature-dependent relaxations to be observed in one experiment.[22] Their performances can be further markedly increased when used in a fractional analytical mode (RMA), allowing progressive isolation of a series of sub-relaxations corresponding to quasi-elementary motions.[20–22]

In order to analyse specific regions of the TSDC spectrum, all these methods were used to some extent, namely TSDC and TSPC global experiments, as well as thermal windowing experiments for RMA analysis. Blocking electrodes (10 μm thick Teflon foils) were used to avoid electrode polarization and injection effects.

It has already been shown that the techniques of polarisation conductivity and TDSC are complementary.[22,23]

Results and Discussion

As proposed by Jonscher,[24,25] the ac conductivity can be written in the form: $\sigma_{ac}(\omega) = \sigma_0 + \sigma'(\omega)$, with $\sigma'(\omega) = A\omega^s$. σ_0 is the diffusive part of the conductivity (*i.e.* the dc conductivity due to the long distance movement of the charge carriers). It corresponds to the limit of σ_{ac} when $\omega \to 0$. The dispersive part of the conductivity, $\sigma'(\omega)$, is a function of the frequency of the applied electric field. It is due to the relaxation of the charge carriers around their equilibrium positions.[26] This movement is equivalent to a dipolar reorientation. The exponent s is a function of temperature and frequency. It generally varies from 0 to 1. The parameter A depends on temperature and frequency.[27]

dc conductivity

When the measuring temperature reaches 80 °C, the dc conductivity of the sample can be determined, whatever the outgassing temperature. The quantity $\ln(\sigma_0 T)$ is plotted as a function of T^{-1}, for different values of T_{og}. The measuring temperatures vary from 80 to 150 °C, whatever the values of T_{og}. The lower limit of 80 °C takes into account the technical limits of the apparatus. Indeed, the impedance-meter has an input impedance of 10 MΩ which does not allow a precise determination of σ_0 when $T < 80$ °C. Fig. 1 shows that $\ln(\sigma_0 T) = f(T^{-1})$ follows an Arrhenius law (in fact Nernst–Einstein law):

$$\sigma_0 = \frac{\sigma_{00}}{T} \exp\left(\frac{-E_{dc}}{kT}\right)$$

E_{dc} being the activation energy and σ_{00}, the pre-exponential factor.

The variation in σ_0 (measured at 80 °C), and E_{dc}, as a function of the number of water molecules per uc n_{H_2O} are reported in Fig. 2 and 3. The dc conductivity shows a minimum (Fig. 2) and then increases regularly. The outgassing temperature is indicated on the two figures. It should be pointed out that the dc conductivity at $T_{og} = 400$ °C is higher than that at $T_{og} = 100$ °C. The activation energy E_{dc} goes through a maximum at $T_{og} = 150$ °C (Fig. 3).

The interpretation of the dc conductivity, and of the dielectric relaxation, supposes that the distribution of the exchangeable cations in the different sites of the network is known. For a given number of Na^+ cations, this distribution depends on the number of adsorbed water molecules and on temperature.[7,8]

The traditional nomenclature of cation sites in faujasite defines their position in relation to the framework of the zeolite.[4] The framework presents large accessible supercages, which represent the useful porosity of faujasite and are con-

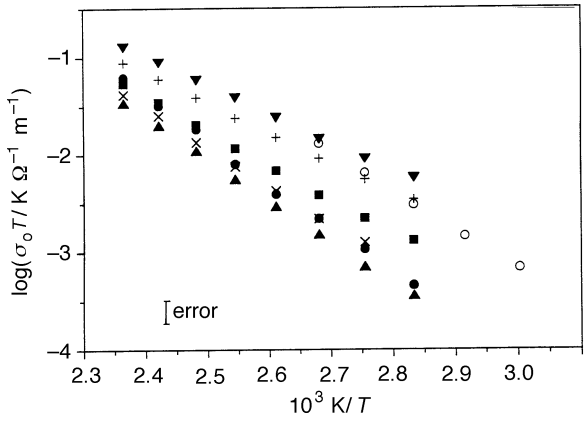

Fig. 1 $\sigma_0 T$ *vs.* T^{-1} for T_{og}: (○) 100, (●) 150, (▲) 200, (×) 250, (■) 300, (+) 350 and (▼) 400 °C

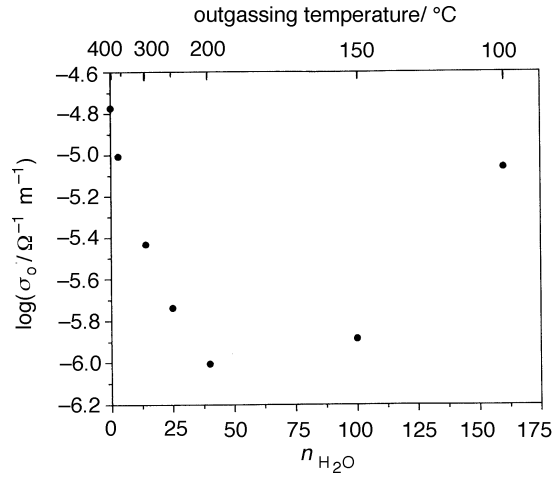

Fig. 2 dc conductivity as a function of the amount of water and the outgassing temperature. Temperature of measurement = 80 °C.

nected to sodalite cages by six-ring (rings formed of six tetrahedra) windows. Cation sites I are located at the centre of the hexagonal prisms, sites I′ on the six-ring between hexagonal prisms and sodalite cages and sites II on the six-ring windows connecting the sodalite cage and the supercage. For the purpose of this paper we consider that a cation coordinated by oxygen atom(s) protruding within the supercage occupies a site III, regardless of the more precise classifications among sites III[28] which have been proposed.

The present knowledge of the position of cations in the cell of hydrated zeolite NaX (88 Na^+ uc^{-1}) can be summarised as follows: 29 Na^+ in sites I or I′, 31 Na^+ in site II (out of 32 possible sites), and at least 23 Na^+ in site III.[28–31] Sodium cations in site I are coordinated by six oxygen atoms of the lattice, in site I′ by three oxygen atoms and by three water molecules within the sodalite cage. Sites I and I′ are mutually exclusive, and can accommodate 32 cations per unit cell. Cations in site II are coordinated by three oxygen atoms of the six-ring window connecting the sodalite cage and supercage and by three water molecules, both in the sodalite cage and the supercage. Cations in site III have been represented as coordinated by one or two oxygen atoms and by five or four, water molecules, respectively, within the supercage.[30,31]

In the cell of the dehydrated form of the zeolite, 32 Na^+ are located in sites I or I′, 32 in site II, and the remaining 24 cations in site III.[28–30] In the dehydration process, some (but not all) cations move from site II to site I. In the dehydrated zeolite, cations are coordinated to lattice oxygens.

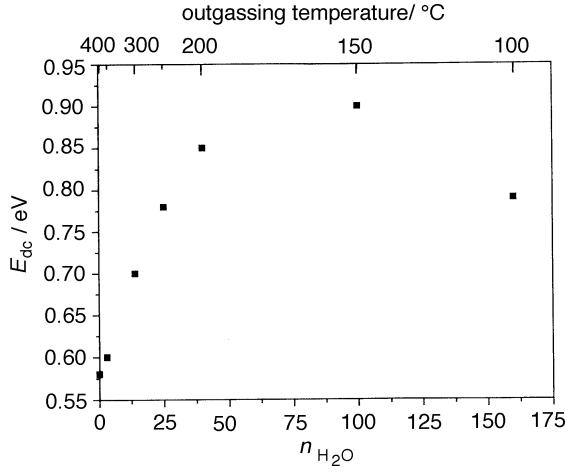

Fig. 3 Activation energy as a function of the amount of water and the outgassing temperature

In the hydrated state, the water can create entities such as $[Na(H_2O)_n]^+$ in the supercage (in the present case $n \leqslant 3$). The dc conductivity should be discussed in terms of Na^+–water dipole interactions. A cell of hydrated zeolite NaX contains up to 250 water molecules. Structural refinement has provided the positions of 162 water molecules, all coordinated to sodium cations.[31] This amount of water corresponds closely to the amount retained in a zeolite partially dehydrated by heating at 100 °C. This effect accounts for the traditional observation of two types of water inside the zeolite lattice.[32]

Al-Ajdah *et al.*[30] determined the position of water molecules at intermediate levels of dehydration. They observed that, when 100 water molecules are left in a zeolite cell (amount left at T_{og} = 150 °C in our conditions), 37 of them are located within the supercage, and that cations in site III are nearly monohydrated. When only 26 water molecules are present, they are distributed in the coordination spheres of cations in site I′ and II, and the cations in site III appear to be fully dehydrated.

In this context, where the dc conductivity decreases with the number of water molecules, the Na^+–network interactions become increasingly predominant compared with Na^+–water dipole interactions. In that case, the conduction mechanism is related to cations on sites III. The result is an increase in the migration energy of the carrier[15] as shown (Fig. 3) by the values of E_{dc} at 100 °C (0.79 eV) and at 150 °C (0.9 eV).

For $T_{og} > 150$ °C, the dc activation energy decreases for increasing T_{og}, and the dc conductivity increases. This can be explained by the fact that there is no longer any water in site III. The water molecules are localized in sites I′ and II. An acceptable mechanism could be the following: during the outgassing process, the increase in the number of potential acceptor sites leads to a decrease in the energy necessary for migration of the cation towards a dehydrated host site (movement of the cation from site II towards sites III or I′). Thus, the activation energy E_{dc} decreases clearly between T_{og} = 150 and 400 °C (0.9 to 0.58 eV).

The value of E_{dc} = 0.58 eV in the anhydrous state is close to those found in several studies.[10,18,33–36] Note that E_{dc} tends towards a constant value when $T_{og} > 350$ °C. This can be explained by the fact that the amount of water remaining in the zeolite after a heat treatment up to 350 °C is very small. The convergence of the results reported by so many authors, using different experimental protocols,[18] shows that grain boundary effects do not really affect the measurements and that the intrinsic properties of the solid can be determined.

To summarise, for $T_{og} < 150$ °C, the conduction is due to cations which are weakly bound, and mainly localized in site III. At 200 °C, these cations are completely dehydrated and water begins to leave the coordination sphere of cations in site II. The cations of site II then move into sites III or I′. The increase in the number of acceptor sites can explain the decrease in the activation energy when T_{og} increases, and consequently the increase in the dc conductivity. The variation in the activation energy E_{dc} with the amount of adsorbed water is consistent with a simple potential barrier model. Indeed, it is well known that the hydration of microporous solids as zeolites (including smectites such as clays) modifies the height of the potential barrier to be crossed by the charge carrier. Macroscopically, this implies a modification of the mobility of the cations.[37–39]

Dielectric relaxation

Fig. 4 shows, for T_{og} = 200 °C, the variation of σ_{ac} as a function of frequency at different temperatures of measurement. The component σ_0 is clearly seen at temperatures higher than 80 °C. The frequency of appearance of the polarization component, $\sigma'(\omega)$, is higher as the measuring temperature is increased. As already mentioned in previous studies,[15,40,41]

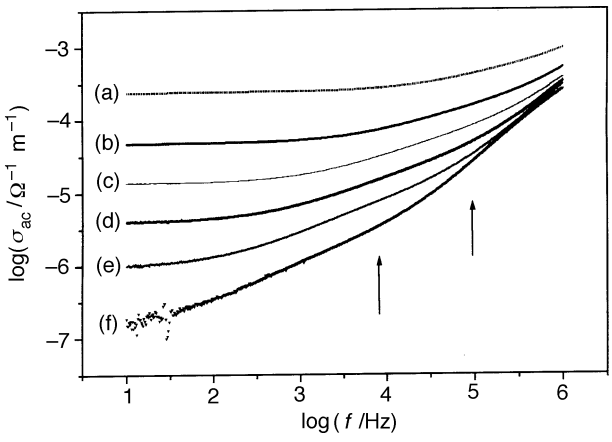

Fig. 4 Frequency dependence of σ_{ac} for measuring temperatures: (a) 170, (b) 140, (c) 120, (d) 100, (e) 80 and (f) 50 °C

two slopes appear clearly when the temperature is lower than 140 °C. They correspond to two dielectric relaxation processes. If we accept the representation of the frequency-dependent conductivity in the form of an Arrhenius law, as proposed by several authors, an activation energy can be evaluated. Of course, this procedure might be debated, but it has been used here in order to compare the present results with those obtained in other studies and eventually assess the limit of such a representation. Fig. 5(a) and (b) show plots of $\sigma_{ac}T = f(T^{-1})$ for two different frequencies, and at different outgassing temperatures, showing that the corresponding activation energies, associated with these two relaxations, can be determined.

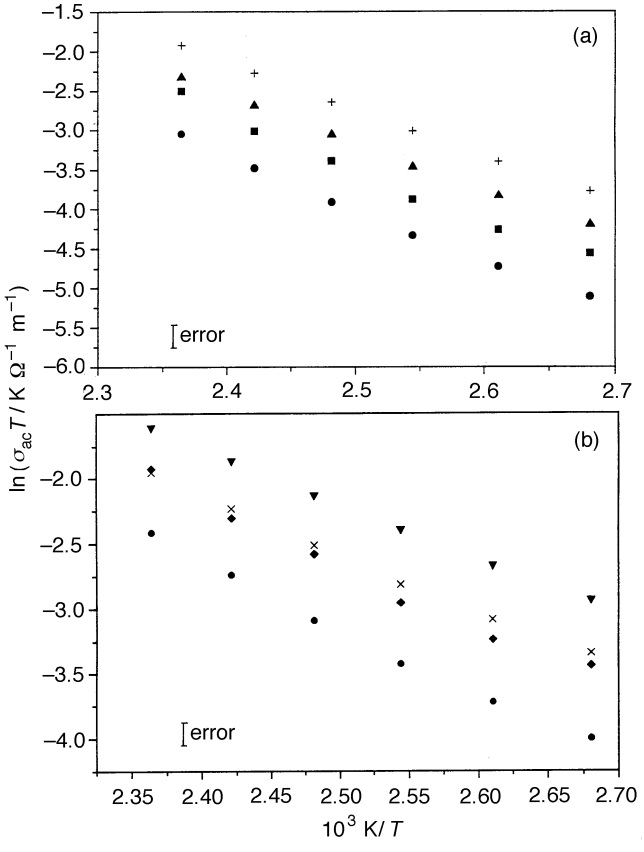

Fig. 5 $\sigma_{ac}T$ *vs.* $1/T$ for T_{og}: (a) (■) 150, (●) 200, (▲) 350 and (+) 400 °C, and (b) (◆) 150, (●) 200, (×) 350 and (▼) 400 °C. f = (a) 10^4 and (b) 10^5 Hz.

The relaxation process is generally ascribed to a local hop of the cation near its site. The relaxation mechanism in zeolites can be described as follows: each site is surrounded by a given number of aluminium atoms, which are coordinated by negatively charged oxygen atoms. The electric neutralisation being incomplete, there is a residual positive charge on the exchangeable cation in its site, and the appearance of a dipole. Thus, the hop of an exchangeable cation towards an empty neighbouring site (with a negative charge) corresponds to a dipole relaxation.

The cations in site III are less bound than those localized in other sites.[42,43] This justified the traditional attribution of the high-frequency (HF) relaxation connected with low energies, to a local hop of the cation in sites III.[15,33,44–46] In a cell of zeolite X, 48 sites III and 96 sites III′ are occupied by 23 Na cations, providing a large availability of empty sites to receive hopping cations. In the anhydrous state, the activation energy of such a process is 0.38 eV (Table 1), which is comparable to the results reported elsewhere for NaX: 0.30,[15] 0.32,[41] 0.35,[46] and 0.42 eV.[33]

The low-frequency (LF) relaxation can be attributed to cations in sites II. Nevertheless, Matron and Jones[33,47] ascribed this LF relaxation to the local hops of cations, and other authors consider that this phenomenon is representative of a Maxwell–Wagner effect.[15,40,41] No proposed explanations for this effect are completely convincing, but the difference in absolute values of the activation energies between the LF and HF processes has to be taken into account.

The value of the LF activation energy corresponding to the dry state (0.52 eV, Table 1) is in agreement with the values of 0.5,[15] and 0.65 eV[33] found in other studies. The variation in σ_{ac} as a function of frequency, at different T_{og} (measuring temperature: 80 °C), is shown in Fig. 6. Two relaxation domains appear clearly when $T_{og} = 150$ and $T_{og} = 200$ °C. Above this outgassing temperature, the component σ_0 is high enough to mask, partly or totally, the LF relaxation. This means that the

Table 1 E_{dc}, E_{ac}(LF) and E_{ac}(HF) as a function of T_{og}

T_{og}/°C	E_{ac}(LF)/eV[a]	E_{ac}(HF)/eV[a]	E_{dc}/eV[a]
150	0.61	0.48	0.9
200	0.59	0.49	0.85
250	0.59	0.48	0.78
300	0.58	0.47	0.70
350	0.53	0.41	0.60
400	0.52	0.38	0.58

[a] ± 0.02 eV.

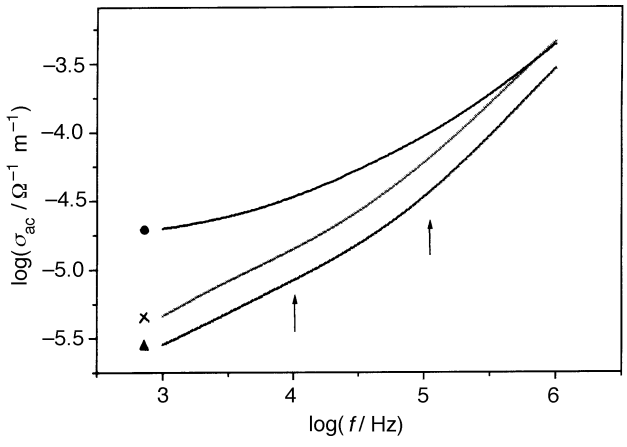

Fig. 6 Frequency dependence of σ_{ac} at T_{og}: (×) 150, (▲) 200 and (●) 400 °C. Temperature of measurement = 80 °C.

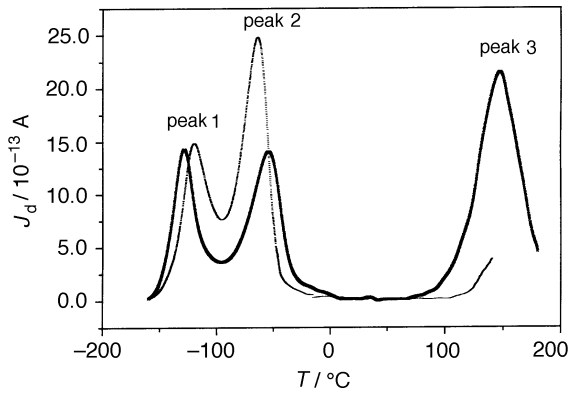

Fig. 7 Depolarization current, J_d, as a function of temperature. T_{og}: (·····) 400 and (——) 170 °C.

activation energy E_{ac} connected to the relaxation of cations of sites II is near to that of the dc conductivity (Table 1). These results are in agreement with those presented by Jansen *et al.*[15]

TSDC

The samples were polarized at $T_p = 150$ °C. The progressive heating leads to the appearance of the depolarization current J_d as a function of temperature.

The variations in J_d as a function of temperature, for two values of T_{og} (170 and 400 °C), are shown in Fig. 7. When there is no space charge, the TSDC and TSPC peaks are characterized by the same position, height and shape, only their directions are opposite; this is a clear indication of the dipolar nature of the process involved.[21,22,48] In this context, peak 3 ($T_{og} = 170$ °C) is probably due to space charges (high-temperature position) and therefore will not be discussed here.

For $T_{og} = 400$ °C, the peak located at relatively high temperature ($T > 140$ °C), is not completely defined since the temperature cannot exceed the temperature of polarization (T_p). In the two cases, only peaks 1 and 2 can be assigned to the cation relaxation of two energetically different sites.

This result is consistent with those obtained in conductivity. The two peaks at relatively low temperature (peaks 1 and 2) can be ascribed to the relaxation of cations located in two different sites. The distribution of activation energies has been determined from windowing experiments and RMA analysis. The TSDC peak can be deconvoluted by the 'thermal-windowing' technique,[20–22] which consists of polarizing only a fragment of the full spectrum of relaxation and depolarizing it partially to isolate a single relaxation process. By varying the value of the temperature of polarization T_p and repeating the process over the entire range, the elementary modes can be isolated one by one. This unique feature of the TSDC method allows the elementary relaxation and activation energies to be determined. The details of the method have been reported elsewhere (see *e.g.* ref. 21). The values of the energies referring to the maximum of peak 1 are 0.4 eV ($T_{og} = 170$ °C) and 0.43 eV ($T_{og} = 400$ °C). The corresponding values for peaks 2 are 0.6 eV ($T_{og} = 170$ °C) and 0.53 eV ($T_{og} = 400$ °C). Peak 1, of relatively low energy, corresponds to the relaxation of cations placed in site III and peak 2 to relaxation of site II.

Conclusion

It has been shown that the dc conductivity and the polarization conductivity of the zeolite NaX are due to exchangeable cations in supercages. The activation energies related to the two relaxation processes are weaker than those obtained with dc measurements. This difference is a function of the outgassing temperature. It is expressed by a large modification of the values of E_{dc} when T_{og} varies (0.9 and 0.58 eV). The migration mechanism is complex. It can be split into two parts: (1) when $T_{og} < 150$ °C, there is a decrease in the dc activation energy owing to dehydration of sites III; (2) when $T_{og} > 150$ °C water located in sites I and II disappears progressively, leading to an increase in E_{dc}.

The relaxation phenomena are ascribed to the relaxation of Na^+ in two different sites: (1) in site II for the LF relaxation, (2) in sites III for the HF relaxation. These phenomena correspond to local hops of cations between sites II and neighbouring sites III (LF) and between neighbouring sites III (HF). The energies associated with these two relaxations depend on the degree of dehydration.

References

1 J. M. Thomas, in *Zeolites: Facts, Figures, Future*, ed. P. A. Jacobs and R. A. Van Santen, Elsevier, Amsterdam, 1989, p. 3.
2 G. A. Ozin, A. Kuperman and A. Stein, *Angew. Chem.*, 1989, **101**, 373.
3 W. M. Meier, D. H. Olson and C. Baerlocker, in *Atlas of Zeolite Structures Types*, Elsevier, London, 1996, p. 104.
4 W. J. Mortier, *Compilation of Extra-framework Sites in Zeolites*, Butterworth, Guilford, 1982, p. 19.
5 A. Chapton, G. Ravalitera, M. Choquet, B. Vandorpe, and L. Gengembre, *Rev. Phys. Appl.*, 1975, **10**, 153.
6 P. Tabourier, J. C. Carru and W. Wacrenier, *J. Chim. Phys.*, 1990, **87**, 43.
7 J. J. Van Dun and W. J. Mortier, *J. Phys. Chem.*, 1988, **92**, 6740.
8 J. J. Van Dun, K. Dhaeze, W. J. Mortier and D. E. W. Vaughan, *J. Phys. Chem. Solids*, 1989, **50**, 469.
9 O. Vigil, J. Fundora, F. Leccabue, and B. E. Watts, *Phys. Status Solidi*, 1994, **141**, K37.
10 E. Krogh Andersen, I. G. Krogh Andersen, J. Metcalf Johansen, K. E. Simonsen and E. Skou, *Solid State Ionics*, 1988, **28–30**, 249.
11 K. E. Simonsen and E. Skou, in *Solid State Protonic Conductors*, ed. J. B. Goodenough, J. Jensen and M. Kleitz, Odense University Press, Odense, Denmark, 1983.
12 H. E. Rabinowitsch and W. C. Wood, *Electrochemistry*, 1933, **39**, 562.
13 D. N. Stamires, *J. Chem. Phys.*, 1962, **36**, 3174.
14 I. R. Beattie and A. Dyer, *J. Chem. Soc., Faraday Trans.*, 1957, **53**, 61.
15 F. J. Jansen and R. A. Schoonheydt, *J. Chem. Soc., Faraday Trans.*, 1973, **69**, 1338.
16 E. Krogh Andersen, I. G. Krogh Andersen, E. Skou and S. Yde-Andersen, *Solid State Ionics*, 1986, **18/19**, 1170.
17 N. Knudsen, E. Krogh Andersen, I. G. Krogh Andersen and E. Skou, *Solid State Ionics*, 1989, **35**, 51.
18 D. C. Freeman and D. Stamires, *J. Chem. Phys.*, 1961, **35**, 799.
19 J. C. Giuntini, A. Jaboker and J. V. Zanchetta, *Clay. Miner.*, 1985, **20**, 347.
20 J. P. Ibar, *Fundamentals of Thermally Stimulated Current, and Relaxation Map Analysis*, ed. SLP Press, New York, 1993.
21 J. Vanderschueren and J. Gasiot, *Thermally Stimulated Current*, ed. P. Braunlich, Springer, Verlag, Berlin, 1979.
22 J. C. Giuntini, J. Vanderschueren, J. V. Zanchetta and F. Henn, *Phys. Rev. B*, 1994, **50**, 12489.
23 G. Chabanis, V. Mouton, A. Abdoulaye, J. C. Giuntini and J. V. Zanchetta, *Ionics*, 1995, **1**, 177.
24 A. K. Jonscher, *Nature (London)*, 1977, **267**, 673.
25 A. K. Jonscher, *Dielectric Relaxation in Solids*, Chesla Dielectric, London, 1983.
26 F. Buet, J. C. Giuntini, F. Henn and J. V. Zanchetta, *Philos. Mag. B*, 1992, **66**, 77.
27 F. Salam, J. C. Giuntini, S. S. Soulayman and J. V. Zanchetta, *Appl. Phys. A*, 1996, **63**.
28 D. H Olson, *Zeolites*, 1995, **15**, 439.
29 Y. I. Smolin, Y. F. Shepelev, I. K. Butikova and V. P. Pentranovskii, *Kristallografiya*. 1983, **28**, 36.
30 G. N. D. Al-Ajdah, A. A. Al-Rished, B. Beagley, J. Dwyer, F. R. Fitch and T. K. Ibrahim, *J. Inclusion Phenom.*, 1985, **3**, 135.
31 G. Calestani, G. Bacca and G. D. Andreetti, *Zeolites*, 1987, **7**, 54.
32 O. Glemser, *Z. Anorg. Chem.*, 1944, **252**, 305.
33 W. Marton, G. Ebert and F. H. Müller, *Kolloid–Z.Z., Polym.*, 1971, **248**, 986.
34 J. Kjaer and E. Skou, *Solid State Ionics*, 1990, **40/41**, 121.
35 N. Cvjeticanin, S. Mentus and N. Petranovic, *J. Chem. Soc., Faraday Trans.*, 1991, **79**, 779.
36 R. Schoonheydt and J. B. Utterhoeven, *Clay Miner.*, 1969, **8**, 71.

37 F. J. Fripiat, A. Jelli, G. Poncellet and J. André, *J. Phys. Chem.*, 1965, **69**, 185
38 R. Prost and J. Chaussidon, *Clay Miner.*, 1969, **8**, 143.
39 P. Pissis and D. Daoukaki-Diamanti, *J. Chem. Solids*, 1993, **54**, 701.
40 R. Schoonheydt and W. De Wilde, *J. Chem. Soc., Faraday Trans.*, 1974, **70**, 2132.
41 U. Lohse, H. Stach, H. Hollnagel and W. Schirmer, *Monatsber. Deutsche Akad. Wissenschaften Berlin*, 1970, **12**, 819.
42 K. T. No, H. Chon, T. Ree and M. S. John, *J. Phys. Chem.*, 1981, **85**, 2065.
43 E. Dempsey, *J. Phys. Chem.*, 1969, **73**, 3660.
44 L. Broussard and D. P. Shoemaker, *J. Am. Chem. Soc.*, 1960, **82**, 1041.
45 R. A. Schoonheydt, *J. Phys.*, 1980, **6-41**, 261.
46 J. C. Carru, P. Tabourier and J. M. Wacrenier, *J. Chim. Phys.*, 1991, **88**, 307.
47 G. Jones, *J. Chem. Soc., Faraday Trans.*, 1985, **71**, 2085.
48 S. W. S. McKerva and M. M. Hughes, *J. Phys. D*, 1975, **8**, 1520

Paper 7/03702C; *Received* 28*th May*, 1997